

# Degradation of 2,4-dichlorophenol in aqueous solution by a hybrid oxidation process

X. Z. Li<sup>1\*</sup>, B. X. Zhao<sup>1,2</sup>, P. Wang<sup>2</sup>

<sup>1</sup>Department of Civil and Structural Engineering, The Hong Kong Polytechnic  
University, Hong Kong, China

<sup>2</sup>School of Municipal and Environmental Engineering, Harbin Institute of Technology,  
Harbin 150090, China

---

## Abstract

A hybrid photo-electro-reaction system has been developed in this study, which consists of three functional electrodes: a TiO<sub>2</sub>/Ti sheet as the anode, a steel (Fe) sheet as another anode in parallel, and a piece of graphite felt (GF) as the cathode. While an electrical current is applied between the Fe anode and GF cathode and UV light is irradiated on the surface of TiO<sub>2</sub>/Ti anode, both of E-Fenton reaction and photoelectrocatalytic (PEC) reaction are involved simultaneously. The integration of E-Fenton and PEC reactions was evaluated in terms of 2,4-dichlorophenol (2,4-DCP) degradation in aqueous solution. In the meantime, the current distribution between two anodes and pH influence on the 2,4-DCP degradation were studied and optimized. Experimental results confirmed that 2,4-DCP in aqueous solution was successfully degraded by 93% and mineralized by 78% within 60 min in such a hybrid oxidation process. When a current intensity of 3.2 mA was applied, the current efficiency for H<sub>2</sub>O<sub>2</sub> generation on the GF cathode was determined to be 61%. Furthermore, the experiments demonstrated that combination of E-Fenton reaction with photocatalytic reaction let the process be less pH sensitive and would be more favorable to water and wastewater treatment in practice.

*Keywords:* E-Fenton; H<sub>2</sub>O<sub>2</sub>; Photocatalysis; TiO<sub>2</sub>; 2,4-DCP; Graphite felt

---

---

\* Corresponding author: Tel: (852) 2766 6016; Fax: (852) 2334 6389; Email: [cexzli@polyu.edu.hk](mailto:cexzli@polyu.edu.hk)

## 31 1. Introduction

32  
33 2,4-Dichlorophenol (2,4-DCP) is a chemical precursor for manufacture of a  
34 widely used herbicide 2,4-dichlorophenoxy acetic acid (2,4-D). After the herbicide  
35 have been applied on agricultural sites, 2,4-DCP is the major transformation product  
36 of 2,4-D by solarphotolysis and/or microbial activities in the nearby soil [1] or in  
37 natural water [2]. 2,4-DCP has also been found in disinfected water after chlorination,  
38 in the flue gas of municipal waste incineration [3], or in pulp and paper wastewater  
39 [4]. It has been realized that 2,4-DCP may cause some pathological symptoms and  
40 changes to endocrine systems of human [5,6].

41 Photocatalysis (PC) is a promising technique of advanced oxidation processes and  
42 has been proven to be successful in purification of water and wastewater [7-9].  
43 However, the quick recombination between excited electrons and holes ( $e^-/h^+$ ) from  
44  $TiO_2$  catalyst results in a low quantum yield of below 5% only. Recently,  
45 photoelectrocatalysis (PEC) demonstrated great attraction in research to further  
46 accelerate PC reaction [10,11] by applying an external potential to drive away the  
47 conduction band electrons from  $TiO_2$  photoanode to a counter electrode as a cathode.  
48 This is an efficient way to eliminate the recombination of  $e^-/h^+$  pairs and results in the  
49 extension of hole's lifetime [12,13].

50 On the other hand, Fenton reaction is also a well-proved technique to oxidize  
51 organic pollutants from water and wastewater effectively, in which hydrogen peroxide  
52 ( $H_2O_2$ ) is catalyzed by ferrous ions ( $Fe^{2+}$ ) to produce hydroxyl radicals ( $HO\cdot$ ). Recent  
53 development has been focused on the generation of  $H_2O_2/Fe^{2+}$  by electrochemical  
54 means named the electro-Fenton (E-Fenton) process. In such a E-Fenton process,  
55 while  $Fe^{2+}$  can be electrically generated on a sacrificial anode via oxidation of iron,  
56  $H_2O_2$  is generated on a carbon cathode via the two-electron reduction of sparged  
57 oxygen [14,15]. Since the efficiency of  $H_2O_2$  generation on the cathode is a key factor  
58 to affect the performance and operating cost in practical application, a variety of  
59 cathode materials such as mercury pool [16], carbon felt [17], reticulated vitreous  
60 carbon [18], graphite [19], activated carbon fiber [20], or carbon-PTFE [21] have been

61 studied. It should be noted that the Fenton reaction is not a universal solution and has  
62 two apparent limits of pH restriction and reaction selectivity, as an efficient reaction  
63 rate only occurs in a narrow pH range of 2-4 and many chemicals such as acetic acid,  
64 acetone, carbon tetrachloride, methylene chloride, *n*-paraffins, maleic acid, malonic  
65 acid, oxalic acid, and trichloroethane etc. are refractory towards Fenton reagent and  
66 [22].

67 Due to the similarity of reaction mechanism utilizing hydroxyl radicals to destroy  
68 organics in aqueous solution between the PEC reaction and E-Fenton reaction, it  
69 would be a good approach to combine them together to be a more efficient process. In  
70 the meantime, some of the drawbacks of each technique might be eliminated by some  
71 characteristics of another technique. The research work presented in this paper has  
72 developed a hybrid process by combination of PEC reaction and E-Fenton reaction in  
73 a three-electrode reaction system, in which 2,4-DCP was used as a model chemical in  
74 aqueous solution and its degradation under different reaction conditions was studied.  
75 Furthermore, the reaction mechanism relevant to the interaction between PEC reaction  
76 and E-Fenton reaction was also discussed based on the experimental results.

77

## 78 **2. Experimental**

### 79 *2.1. Preparation of three electrodes*

80 Titanium sheet (purity: 99.6%; thickness: 0.14 mm) from Goodfellow Cambridge  
81 Ltd. was used as a raw material to prepare a TiO<sub>2</sub>/Ti film electrode. A piece of Ti  
82 sheet (10 mm × 50 mm) was ultrasonically cleaned in alcohol and acetone solutions,  
83 respectively and then washed with distilled water. The cleaned Ti sheet was  
84 submerged in 2 M HF solution for 2 min to polish its surface chemically. An anodic  
85 oxidation process at low voltage was conducted in a dual-electrode reaction chamber,  
86 in which the cleaned Ti sheet was used as the anode and a Pt foil with the same size  
87 was applied as the cathode. Two electrodes were submerged in aqueous electrolyte  
88 solution (1.5 M H<sub>3</sub>PO<sub>4</sub> and 0.3 M HF) and an electrophoresis power supply (EPS  
89 600 Pharmacia Biotech) was used to provide electrical potentials/currents between  
90 two electrodes. The anodic oxidation process was conducted in two stages for about

91 30 min. In the first stage, a constant current density of  $10 \text{ mA cm}^{-2}$  was fixed, until  
92 voltage gradually increased up to 30 V (galvanostatic anodization). In the second  
93 stage, the constant voltage of 30 V was kept to allow the current density was gradually  
94 reduced (potentiostatic anodization) until the oxidation reaction was complete. Then  
95 the anodized  $\text{TiO}_2/\text{Ti}$  sheet was calcinated at 723 K for 2 h for further phase  
96 transformation and crystallization. A piece of rectangle stainless steel sheet ( $10 \text{ mm} \times$   
97  $50 \text{ mm} \times 1 \text{ mm}$ ) after surface passivation pretreatment was simply used as an iron (Fe)  
98 electrode. A piece of graphite fiber (GF) about 2 mm thick supplied by US National  
99 Electrical Carbon Products Inc. was cut into the same size ( $10 \text{ mm} \times 50 \text{ mm}$ ) as a GF  
100 electrode without any further treatment.

101

## 102 *2.2. A three-electrode photoreactor and experimental procedure*

103 A novel three-electrode ( $\text{TiO}_2\text{-Fe-GF}$ ) photoreactor system used in this study  
104 consists of a cylindrical quartz glass reactor with a three-electrode configuration and  
105 an 8-W medium-pressure mercury lamp (LZC-UVA-365, Canada) with a main  
106 emission at 365 nm as an external UV-A light source. In this reactor, while the GF  
107 electrode was used as the cathode to generate  $\text{H}_2\text{O}_2$ , the  $\text{TiO}_2/\text{Ti}$  electrode was  
108 employed as the first anode to conduct PEC reaction under UV-A illumination and the  
109 Fe electrode was used as the second anode in parallel to release ferrous ion ( $\text{Fe}^{2+}$ )  
110 continuously for E-Fenton reaction. In addition, a saturated calomel electrode (SCE)  
111 was also placed in a separate chamber for potential control. In such a  $\text{TiO}_2\text{-Fe-GF}$   
112 photoreactor, the working current and potential on the GF cathode were controlled by  
113 a potentiostat (ZF-9, Shanghai, China) and the current distribution between two  
114 anodes ( $\text{TiO}_2/\text{Ti}$  and Fe) was controlled by an external variable resistor.

115

116 [Fig. 1]

117

118 2,4-DCP chemical was purchased from Aldrich with analytical grade. Aqueous  
119 2,4-DCP solution was prepared by dissolving 2,4-DCP into aqueous electrolyte  
120 solution ( $0.02 \text{ M Na}_2\text{SO}_4$ ). During each reaction, 50 mL of the 2,4-DCP solution was  
121 continuously aerated by oxygen and an electrical current was applied between the

122 anodes and cathode. Samples were taken from the reaction solution at different time  
123 intervals for analyses. Prior to HPLC analysis, all samples were filtered by a 0.45  $\mu\text{m}$   
124 Millipore filter to remove any particulates including the fiber desquamation from GF  
125 electrode. During the reaction, 50 mL reaction solution was continuously aerated by  
126 an oxygen gas flow at 40 mL  $\text{min}^{-1}$ , which was sufficient for oxygen supply and  
127 mixing.

128

### 129 2.3. Analytical methods

130 2,4-DCP concentration was determined by high performance liquid  
131 chromatograph (HPLC Finnigan P4000 Model) equipped with a UV detector  
132 (UV6000LP). The separation column is a reverse-phase column (RESTEK Pinnacle  
133 II, d-C18 4.6 mm  $\times$  250 mm, 5  $\mu\text{m}$ ) and a mobile phase consists of  
134 acetonitrile:water:acetic acid (69:30:1).  $\text{H}_2\text{O}_2$  concentration was measured by a  
135 spectrophotometer (GENESYS 2 UV-VIS) at 400 nm wavelength, using  $\text{K}_2\text{Ti}(\text{C}_2\text{O}_4)_3$   
136 (analytical grade) as a colored indicator. Dissolved organic carbon (DOC)  
137 concentration was measured by a TOC analyzer (Shimadzu TOC-5000A) after sample  
138 filtration using the 0.45 (m Millipore filter.

139

## 140 3. Results and discussion

141

### 142 3.1. Effect of current intensity on $\text{H}_2\text{O}_2$ generation

143 The GF cathode used in this study is a carbon material with a microporous  
144 structure and high reduction potential, which can generate  $\text{H}_2\text{O}_2$  on its surface with  
145 the following reaction:

146



148

149 The rate of  $\text{H}_2\text{O}_2$  generation on the GF cathode depends on several factors  
150 including electrolyte properties, applied current intensity, and dissolved oxygen  
151 concentration in the reaction solution. To study the rate of  $\text{H}_2\text{O}_2$  generation affected  
152 by current intensity as a main parameter, a set of experiments in aqueous 0.02 M

153 Na<sub>2</sub>SO<sub>4</sub> solution (without 2,4-DCP) was conducted by applying different current  
154 intensity from 0.5 mA to 5.0 mA between the Pt anode and the GF cathode. Each  
155 experiment lasted for 150 min and samples were taken at different time intervals to  
156 determine the accumulative H<sub>2</sub>O<sub>2</sub> concentration in the solution. The experimental  
157 results are shown in Fig. 2.

158

159 [Fig. 2]

160

161 It can be seen that H<sub>2</sub>O<sub>2</sub> concentration in the Na<sub>2</sub>SO<sub>4</sub> solution gradually built up  
162 along with reaction time and eventually approached to its maximum levels. The  
163 experimental results showed that the higher current intensity was applied, the higher  
164 H<sub>2</sub>O<sub>2</sub> concentration was achieved. For example, the accumulative H<sub>2</sub>O<sub>2</sub> concentration  
165 at 60 min was increased from 0.125 mM at 0.5 mA to 0.728 mM at 3.2 mA  
166 significantly and was further increased up to 0.836 at 5.0 mA. To evaluate the current  
167 efficiency of H<sub>2</sub>O<sub>2</sub> generation on the cathode, it is assumed that H<sub>2</sub>O<sub>2</sub> is electrically  
168 generated from oxygen in aqueous solution with a theoretical amount determined by  
169 the following equation:

170

$$171 \quad Q = I \times t = 2n \times N_A \times e = 2n \times (6.02 \times 10^{23}) \times (1.60 \times 10^{-19})$$

172

173 where  $Q$  is total quantity of electricity in coulombs (C);  $t$  is reaction time (s) and  $I$  is  
174 current intensity (A);  $n$  is the moles of electrogenerated H<sub>2</sub>O<sub>2</sub> (M);  $N_A$  is Avogadro's  
175 constant ( $6.02 \times 10^{23}$  molecules/mole); and  $e$  is electron charge ( $1.60 \times 10^{-19}$  C).

176 According the above equation, the theoretical amount of H<sub>2</sub>O<sub>2</sub> at different current  
177 intensity for the reaction time at 60 min was calculated and the current efficiency of  
178 H<sub>2</sub>O<sub>2</sub> generation is evaluated as listed in Table 1. It can be seen that the efficiency of  
179 H<sub>2</sub>O<sub>2</sub> generation on the GF cathode is decreased from 67% to 45% with the increased  
180 current intensity from 0.5 mA to 5.0 mA. Since the efficiency was quickly declined  
181 from 61% to 45% at the current intensity higher than 3.2 mA, the current intensity of  
182 3.2 mA was employed in the following experiments as a cost-effective condition.

183

184 [Table 1]

185

### 186 3.2. Current distribution between two anodes

187 In this three-electrode photoreactor, two anodes (TiO<sub>2</sub>/Ti and Fe) were applied in  
188 parallel. While a total current intensity of 3.2 mA was applied on the GF cathode to  
189 generate H<sub>2</sub>O<sub>2</sub> sufficiently, the division of the current between two anodes was  
190 controlled by the external variable resistor. A set of experiments at different ratios of  
191 Fe:TiO<sub>2</sub>/Ti (3.2:0, 3.1:0.1, 3.0:0.2, 2.6:0.6, and 1.8:1.4) was conducted in aqueous  
192 2,4-DCP solution with an initial concentration of 15 mg L<sup>-1</sup> under UV-A illumination  
193 for 60 min and the experimental results are shown in Fig. 3. The experiments  
194 demonstrated that the 2,4-DCP degradation reaction was affected by current  
195 distribution between two anodes significantly and the fastest degradation was  
196 achieved by nearly 90% at the ratio of 3.1:1.0 (3.1 mA on the Fe anode and 0.1 mA on  
197 the TiO<sub>2</sub>/Ti anode). These results indicate that a small current on the TiO<sub>2</sub>/Ti anode is  
198 sufficient to enhance the photocatalytic reaction and also avoid any electro-corrosion  
199 of the TiO<sub>2</sub>/Ti electrode. On the other hand, a higher current on the Fe anode can  
200 release more ferrous ions into the reaction solution to enhance the E-Fenton reaction.

201

202 [Fig. 3]

203

### 204 3.3. Interaction of individual reactions

205 In such a hybrid reaction system, several reactions could contribute to the  
206 2,4-DCP degradation in aqueous solution, including (1) direct photolysis by UV-A  
207 illumination, (2) direct electro-chemical oxidation on the TiO<sub>2</sub>/Ti anode or Fe anode,  
208 (3) PEC reaction and H<sub>2</sub>O<sub>2</sub>-assisted PEC reaction on the TiO<sub>2</sub>/Ti electrode, and (4)  
209 E-Fenton reaction and photo-assisted E-Fenton reaction in the solution. Since the  
210 photolysis of 2,4-DCP under UV-A irradiation is insignificant due to low adsorption  
211 band of below 286 nm by 2,4-DCP [23] and the direct electro-chemical oxidation on  
212 both anodes is also weak due to a low current intensity of 3.2 mA only. Comparatively  
213 both the H<sub>2</sub>O<sub>2</sub>-assisted PEC reaction and photo-assisted E-Fenton reaction may play

214 more important roles. To study the interaction of individual reactions, three  
215 experiments were conducted. The first experiment was carried out using two  
216 electrodes only (TiO<sub>2</sub>/Ti anode and GF cathode). The experiment was performed in  
217 the 2,4-DCP solution (initial concentration = 15 mg L<sup>-1</sup>) under UV-A illumination by  
218 applying a weak current at 0.1 mA as a H<sub>2</sub>O<sub>2</sub>-assisted PEC oxidation reaction. The  
219 second experiment was conducted using two electrodes (Fe anode and GF cathode)  
220 and a high current at 3.1 mA was applied with and without UV-A illumination as  
221 photo-assisted E-Fenton and E-Fenton reactions. The third experiment was conducted  
222 using three electrodes together (TiO<sub>2</sub>/Ti anode, Fe anode and GF cathode) and a total  
223 current intensity of 3.2 mA with a distribution ratio of 3.1:0.1 was applied. The  
224 experiment was performed under UV-A illumination to represent an integrative  
225 oxidation reaction. All the above experiments with an initial pH 5.8 lasted for 60 min.  
226 and the experimental results are compared in Fig. 4.

227

228 [Fig. 4]

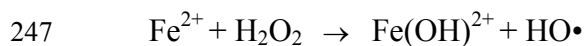
229

230 The experimental results showed that the 32% of 2,4-DCP reduction was achieved  
231 by the E-Fenton reaction after 60 min; 45% by the photo-assisted E-Fenton reaction;  
232 and 46% by the H<sub>2</sub>O<sub>2</sub>-assisted TiO<sub>2</sub> PEC reaction. These results confirmed that both  
233 the TiO<sub>2</sub> PEC reaction and E-Fenton reaction played significant roles in the 2,4-DCP  
234 degradation. These results also confirmed that the 2,4-DCP degradation by E-Fenton  
235 reaction was really enhanced by UV-A illumination. Furthermore, much higher  
236 percent of 2,4-DCP reduction up to 93% was achieved by the integrative reaction, in  
237 which the proper current distribution with the ratio of 3.1:0.1 can well balance both  
238 reactions in such a three-electrode reaction system. In such a reaction system, while  
239 the existence of H<sub>2</sub>O<sub>2</sub> in the solution could enhance the TiO<sub>2</sub> PEC reaction as the  
240 H<sub>2</sub>O<sub>2</sub>-assisted TiO<sub>2</sub> PEC reaction and UV-A illumination could also enhance the  
241 E-Fenton reaction as the photo-assisted E-Fenton reaction, where some interactive  
242 reactions may occur as well. It has been reported that Fe(OH)<sup>2+</sup> has an absorption  
243 band between 290 and 400 nm and can produce hydroxyl radicals and Fe(II) ions. The

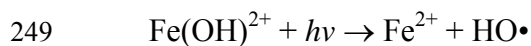


244 primary reactions in the case of photo-Fenton reaction using the near-UV and even  
245 visible light can be given as follows [24]:

246



248



250

251 To further compare the rates of 2,4-DCP reduction in the above experiments, all  
252 experimental data were fitted by the simple first-order kinetic model, the values of  
253 kinetic constant,  $k$ , for all reactions were calculated and are presented in Table 2. It  
254 can be noted that both constants of  $\text{H}_2\text{O}_2$ -assisted PEC reaction and photo-assisted  
255 E-Fenton reaction are 1.01 and 1.11, respectively, while the constant of the integrative  
256 reaction is 4.23. These results demonstrated that the  $\text{H}_2\text{O}_2$ -assisted PEC reaction and  
257 photo-assisted E-Fenton reaction were two main reactions dominating in such a  
258 three-electrode reaction system. However, the rate of integrative reaction was even  
259 higher than the sum of  $\text{H}_2\text{O}_2$ -assisted PEC reaction and photo-assisted E-Fenton  
260 reaction. It should be indicated that any extra benefits obtained from the combination  
261 of photochemical reaction and electrochemical reaction would be more attractive  
262 rather than the simple summation only. However, the exact mechanism of individual  
263 reactions involved in such a three-electrode reaction system is quite sophisticated and  
264 needs to be further explored in the following studies.

265

266 [Table 2]

267

### 268 *3.4. Effect of pH on 2,4-DCP degradation*

269 Since E-Fenton reaction is a pH-sensitive approach, the effect of pH on 2,4-DCP  
270 degradation is studied by conducting three experiments for the  $\text{H}_2\text{O}_2$ -assisted  $\text{TiO}_2$   
271 PEC reaction, the E-Fenton reaction, and the integrative reaction, respectively in a  
272 wide pH range of 1-9. The reaction at pH 1 was controlled with  $\text{H}_2\text{SO}_4$ - $\text{H}_3\text{PO}_4$  buffer  
273 solution and the reactions at pH 3-9 are controlled with  $\text{H}_3\text{PO}_4$ - $\text{NaH}_2\text{PO}_4$ - $\text{Na}_2\text{HPO}_4$

274 buffer solution. The experimental results are shown in Fig. 5.

275

276 [Fig. 5]

277

278 The first experiment demonstrated that pH had a moderate influence on the  
279  $\text{H}_2\text{O}_2$ -assisted  $\text{TiO}_2$  PEC reaction, in which 2,4-DCP degradation was increased with  
280 increased pH from 1 to 7 gradually and then decreased beyond pH 7 slightly. The  
281 second experiment confirmed that pH had a sharp influence on the E-Fenton reaction  
282 with a maximum reaction rate at pH 2.5-3 as a common nature of most Fenton  
283 reactions. Furthermore, the third experiment showed that the 2,4-DCP degradation in  
284 the integrative reaction was increased quickly at the lower pH range from 1 to 3 and  
285 then gradually decreased at the higher pH range from pH 3 to 9. However, the  
286 reduction of 2,4-DCP degradation from its maximum value at pH 3 to the lowest  
287 value at pH 9 was only 10% difference. From these results, it is believed that the  
288 combination of E-Fenton reaction with photocatalytic reaction may gain a benefit to  
289 overcome its pH-sensitive character and it becomes less necessary to adjust pH of  
290 water and wastewater with a neutral pH condition prior to the treatment.

291 To further study the pH change during the integrative reaction, one more  
292 experiment was conducted without pH control under UV-A illumination for 60 min  
293 with an initial 2,4-DCP concentration of  $15 \text{ mg l}^{-1}$  and initial pH 5.8. The 2,4-DCP  
294 concentration and pH were monitored simultaneously during the reaction. The  
295 experimental results in Fig. 6 demonstrated that when 2,4-DCP degradation was  
296 achieved by more than 90% at 60 min, pH of reaction solution was only slightly  
297 decreased from 5.8 to 4.8. Although several factors may affect the pH in the reaction  
298 solution, it was confirmed in our previous work that the  $\text{H}_2\text{O}_2$  generation on the  
299 cathode can increase pH by consuming  $\text{H}^+$ , while the degradation of some organics  
300 such as 2,4,6-TCP can decrease pH due to release of acidic intermediate products such  
301 as organic acids [25]. Some researchers also reported that degradation of 2,4-DCP  
302 produced weak acids by photo-Fenton-like oxidation [26]. This pH neutralization  
303 function in the  $\text{TiO}_2/\text{Ti-Fe-GF}$  reaction system might have one more benefit to

304 maintain pH for any acid-releasing reactions in practical water and wastewater  
305 treatment.

306

307 [Fig. 6]

308

### 309 *3.5. Accumulation of H<sub>2</sub>O<sub>2</sub> concentration*

310 The H<sub>2</sub>O<sub>2</sub> concentration in the reaction solution plays a critical role, depending on  
311 both rates of its generation and consumption. To study the H<sub>2</sub>O<sub>2</sub> accumulation in the  
312 integrative reaction system, 4 experiments were carried out by applying the same  
313 current intensity of 3.2 mA on the GF cathode under different reaction conditions,  
314 which included two experiments in aqueous 0.02 M Na<sub>2</sub>SO<sub>4</sub> only solution with and  
315 without UV-A illumination and other two experiments in aqueous 2,4-DCP + 0.02 M  
316 Na<sub>2</sub>SO<sub>4</sub> solution with and without UV-A illumination. The experimental results are  
317 summarized in Fig. 7. The results demonstrated that the accumulative H<sub>2</sub>O<sub>2</sub>  
318 concentration in the aqueous 0.02 M Na<sub>2</sub>SO<sub>4</sub> only solution were significantly higher  
319 than those in the 2,4-DCP+0.02 M Na<sub>2</sub>SO<sub>4</sub> solution, due to no H<sub>2</sub>O<sub>2</sub> consumption  
320 resulted from the reaction with 2,4-DCP. On the other hand, the accumulative H<sub>2</sub>O<sub>2</sub>  
321 concentration under UV-A illumination built up slightly slower than those without  
322 UV-A illumination, due to more H<sub>2</sub>O<sub>2</sub> consumption under UV-A illumination.

323

324 [Fig. 7]

325

### 326 *3.6. Mineralization of 2,4-DCP*

327 To study the 2,4-DCP mineralization in the integrative reaction, DOC at different time  
328 intervals was also determined and the experimental results are shown in Fig. 8. The  
329 results showed that the degree of 2,4-DCP mineralization in the integrative reaction  
330 was higher than both the H<sub>2</sub>O<sub>2</sub>-assisted-TiO<sub>2</sub> PEC and photo-assisted E-Fenton  
331 reactions, significantly. It should be noted that 78% of 2,4-DCP mineralization was  
332 achieved by the integrative reaction, which was even higher than 57% as the sum of  
333 H<sub>2</sub>O<sub>2</sub>-assisted-TiO<sub>2</sub> PEC and photo-assisted E-Fenton reactions. Sabhi and Kiwi [23]

334 carried out a similar photo-assisted E-Fenton reaction and found that mineralization of  
335 2,4-DCP was only 21% after 60 min reaction time when added H<sub>2</sub>O<sub>2</sub> concentration  
336 was 1.25mM. Similar to the pattern of 2,4-DCP degradation, the experiments further  
337 confrimed that some interactive reactions might occur in such a TiO<sub>2</sub>/Ti-Fe-GF  
338 reaction system beyond the PEC reaction and E-Fenton reaction, which provided extra  
339 benefits to develop an efficiency treatment process.

340

341 [Fig. 8]

342

#### 343 **4. Conclusion**

344 In this study, it has been confirmed that 2,4-DCP in aqueous solution is  
345 successfully degraded by 93% and mineralized by 78% within 60 min in a hybrid  
346 oxidation process by integrating the E-Fenton and photocatalytic reactions. When a  
347 current intensity of 3.2 mA was applied on the GF cathode, the current efficiency for  
348 H<sub>2</sub>O<sub>2</sub> generation was determined to be 61%. Although the E-Fenton reaction is a  
349 pH-sensitive process, the experiments demonstrated that combination of E-Fenton  
350 reaction with photocatalytic reaction let the process become less pH sensitive and can  
351 be applied under a more neutralized pH condition, which would be favorable to water  
352 and wastewater treatment in practice.

353

#### 354 **Acknowledgements**

355 Authors would thank the Hong Kong Government Research Grant Committee  
356 for a financial support to this work (RGC No: PolyU5148/03E).

#### 357 **References**

- 358 1. M.A. Crespin, M. Gallego, M. Valcarcel, Study of the degradation of the herbicides  
359 2,4-D and MCPA at different depths in contaminated agricultural soil, Environ.  
360 Sci. Technol. 35 (2001) 4265–4270.

- 361 2. A. Lagana, A. Bacaloni, I. De Leva, A. Faberi, G. Fago, A. Marino, Occurrence  
362 and determination of herbicides and their major transformation products in  
363 environmental waters, *Anal. Chim. Acta* 462 (2002) 187–193.
- 364 3. N.V. Heeb, I.S. Dolezal, T. Buhner, P. Mattrel, M. Wolfensberger, Distribution of  
365 halogenated phenols including mixed brominated and chlorinated phenols in  
366 municipal water incineration flue-gas, *Chemosphere* 31 (1995) 3033–3041.
- 367 4. M. Perez, F. Torrades, J.A. Garcia-Hortal, X. Domenech, J. Peral, Removal of  
368 organic contaminants in paper pulp treatment effluents under Fenton and  
369 photo-Fenton conditions, *Appl. Catal. B: Environ.* 36 (2002) 63–74.
- 370 5. A. Handan, O. Nurullah, U. Nuray, Investigation of the accumulation of  
371 2,4-dichlorophenoxyacetic acid (2,4-D) in rat kidneys, *Forensic Sci. Int.* 153,  
372 (2005) 53–57.
- 373 6. J.F. Zhang, H. Liu, Y.Y. Sunb, X.R. Wang, J.C. Wu, Y.Q. Xue, Responses of the  
374 antioxidant defenses of the goldfish *carassius auratus* exposed to  
375 2,4-dichlorophenol, *Environ. Toxicol. Phar.* 19 (2005) 185–190.
- 376 7. M. Bekbolet, G.A. Ozkosemen, A preliminary investigation on the photocatalytic  
377 degradation of a model humic acid, *Water Sci. Res.* 33 (1996) 189–194.
- 378 8. S.D. Richardson, A.D. Thruston, T.W. Collette, K.S. Patterson, B.W. Lykins, J.C.  
379 Ireland, Identification of TiO<sub>2</sub>/UV disinfection by-products in drinking water,  
380 *Environ. Sci. Technol.* 30 (1996) 3327–3334.
- 381 9. B.R. Eggins, F.L. Palmer, J.A. Byrne, Photocatalytic treatment of humic substances  
382 in drinking water, *Water Res.* 31 (1997) 1223–1226.
- 383 10. R.J. Candal, W.A. Zeltner, M.A. Anderson, Effects of pH and applied potential on  
384 photocurrent and oxidation rate of saline solutions of formic acid in a  
385 photoelectrocatalytic reactor, *Environ. Sci. Technol.* 34 (2000) 3443–3451.
- 386 11. J. Luo, M. Hepel, Photoelectrochemical degradation of naphthol blue black diazo  
387 dye on WO<sub>3</sub> film electrode, *Electrochim. Acta* 46 (2001) 2913–2922.
- 388 12. M.V.B. Zanoni, J.J. Sene, M.A. Anderson, Photoelectrocatalytic degradation of  
389 remazol brilliant orange 3R on titanium dioxide thin-film electrodes, *J.*  
390 *Photochem. Photobiol.* 157 (2003) 55–63.

- 391 13. P.A. Carneiro, M.E. Osugi, J.J. Sene, M.A. Anderson, M.V.B. Zanoni, Evaluation  
392 of color removal and degradation of a reactive textile azo dye on nanoporous  
393 TiO<sub>2</sub> thin-film electrodes, *Electrochim. Acta* 49 (2004) 3807–3820.
- 394 14. Q.Q. Wang, A. Lemley, Kinetic model and optimization of 2,4-D degradation by  
395 anodic Fenton treatment, *Environ. Sci. Technol.* 35 (2001) 4509-4514.
- 396 15. E. Brillas, J. Casado, Aniline degradation by electro-Fenton® and  
397 peroxi-coagulation processes using a flow reactor for wastewater treatment,  
398 *Chemosphere* 47 (2002) 241–248.
- 399 16. E. Kusvuran, O. Gulnaz, S. Irmak, O.M. Atanur, H.I. Yavuz, O. Erbatur,  
400 Comparison of several advanced oxidation processes for the decolorization of  
401 reactive red 120 azo dye in aqueous solution, *J. Hazard. Mater.* B109 (2004)  
402 85–93.
- 403 17. M.A. Oturan, J. Peiroten, P. Chartrin, A.J. Acher, Complete destruction of  
404 *p*-nitrophenol in aqueous medium by electro-Fenton method, *Environ. Sci.*  
405 *Technol.* 34 (2000) 3474–3479.
- 406 18. E. Fokedey, A. Van Lierde, Coupling of anodic and cathodic reactions for phenol  
407 electro-oxidation using three-dimensional electrodes, *Water Res.* 36 (2000)  
408 4169–4175.
- 409 19. M. Panizza, G. Cerisola, Removal of organic pollutants from industrial  
410 wastewater by electrogenerated Fenton's reagent, *Water Res.* 35 (2001)  
411 3987–3992.
- 412 20. A.M. Wang, J.H. Qu, J. Ru, H.J. Liu, J.T. Ge, Mineralization of an azo dye acid  
413 red 14 by electro-Fenton's reagent using an activated carbon fiber cathode,  
414 *Dyes Pigments* 65 (2005) 227–233.
- 415 21. B. Boye, M.M. Dieng, E. Brillas, Degradation of herbicide 4-  
416 chlorophenoxyacetic acid by advanced electrochemical oxidation methods,  
417 *Environ. Sci. Technol.* 36 (2002) 3030–3035.
- 418 22. M. Pera-Titus, V. Garcia-Molina, M.A. Banos, J. Gimenez, S. Esplugas,  
419 Degradation of chlorophenols by means of advanced oxidation processes: A  
420 general review, *Appl. Catal. B: Environ.* 47 (2004) 219–256.

- 421 23. S. Sabhi and J. Kiwi, Degradation of 2,4-dichlorophenol by immobilized iron  
422 catalysis, *Wat. Res.* 35 (2001) 1994–2002.
- 423 24. P.R. Gogate, P.R. Pandit, A review of imperative technologies for wastewater  
424 treatment II: hybrid methods, *Adv. Environ. Res.* 8 (2003) 553-597.
- 425 25. X.Z. Li, H.S. Liu, Development of an E-H<sub>2</sub>O<sub>2</sub>/TiO<sub>2</sub> photoelectrocatalytic  
426 oxidation system for water and wastewater treatment, *Environ. Sci. Technol.* 39  
427 (2005) 4614–4620.
- 428 26. W. Chu, C.Y. Kwan, K.H. Chan, A study of kinetic modeling and reaction  
429 pathway of 2,4-dichlorophenol transformation by photo-Fenton-like oxidation,  
430 *Hazard. Mater.* 121 (2005) 119–126.

431

432

433

434

435 Table 1. Accumulative Amount of H<sub>2</sub>O<sub>2</sub> (C<sub>H2O2</sub>) in Experiments and Theoretical  
 436 Values at 60 min.

Applied current intensity (mA)	C <sub>H2O2</sub> (mM)	Theoretical value (mM)	Generation efficiency (%)
0.5	0.125	0.187	67
1.5	0.349	0.56	62
3.2	0.728	1.19	61
5.0	0.836	1.87	45

437

438 Table 2. Kinetic Constant (k<sub>R</sub>) for 2,4-DCP Degradation in Aqueous Solution

Reaction system	k <sub>R</sub> (×100 / min <sup>-1</sup> )	R <sup>2</sup>	Degradation (%)
Anodic oxidation on TiO <sub>2</sub> electrode	0.04	0.9982	2.9
Anodic oxidation on Fe electrode	0.12	0.9929	6.2
Photolysis under UV-A illumination	0.07	0.9971	3.6
E-Fenton reaction	0.62	0.9378	32
TiO <sub>2</sub> PEC reaction	0.81	0.9825	36
H <sub>2</sub> O <sub>2</sub> -assisted TiO <sub>2</sub> PEC reaction	1.01	0.9783	45
Photo-assisted E-Fenton reaction	1.11	0.9779	46
Integrative reaction	4.23	0.9956	93

439

440

441

442

443

444

445

446

447

448

449

450

451

452



453 **List of figure captions**

454

455 Fig.1. Sketch of the photo-electro-reaction system.

456

457 Fig. 2. Effect of current on H<sub>2</sub>O<sub>2</sub> generation (O<sub>2</sub> flow rate = 40 ml min<sup>-1</sup> nearby GF cathode).

458

459 Fig. 3. Effect of current distribution on 2,4-DCP degradation (Anodes: TiO<sub>2</sub>/Ti and Fe; cathode:

460 GF; total current intensity = 3.2 mA; O<sub>2</sub> flow rate = 40 ml min<sup>-1</sup>; initial 2,4-DCP

461 concentration = 15mg l<sup>-1</sup> under UV-A irradiation).

462

463 Fig. 4. 2,4-DCP degradation in aqueous solution by different reactions without pH control

464

465 Fig. 5. Effect of pH on 2,4-DCP degradation by different reactions with pH control.

466

467 Fig. 6. pH change during 2,4-DCP degradation in aqueous solution by integrative reaction without

468 pH control.

469

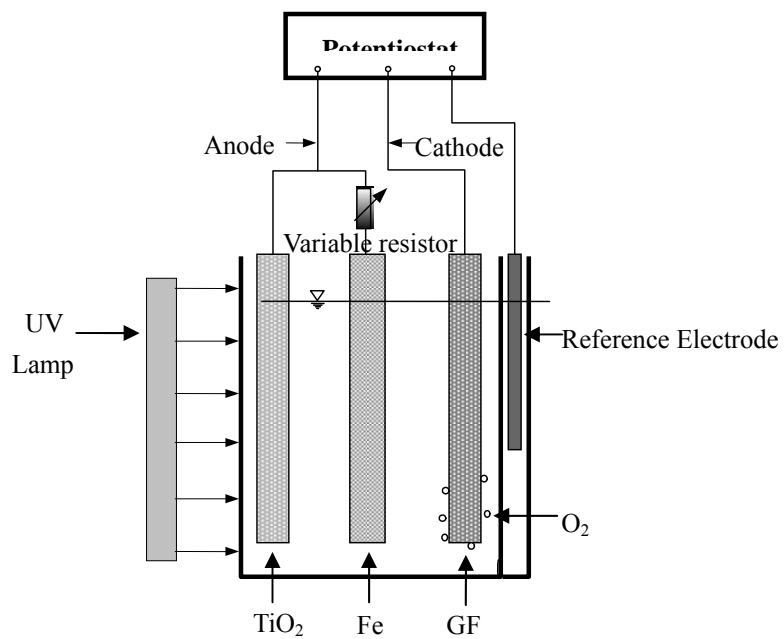
470 Fig. 7. H<sub>2</sub>O<sub>2</sub> accumulation under different experimental conditions without pH control.

471

472 Fig. 8. Mineralization of 2,4-DCP in aqueous solution in different reactions.

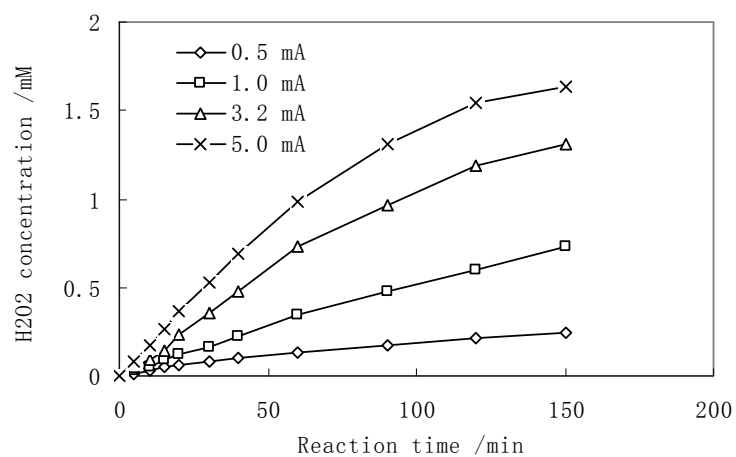
473

474



476  
477  
478  
479  
480  
481  
482 Fig. 1.  
483  
484

485



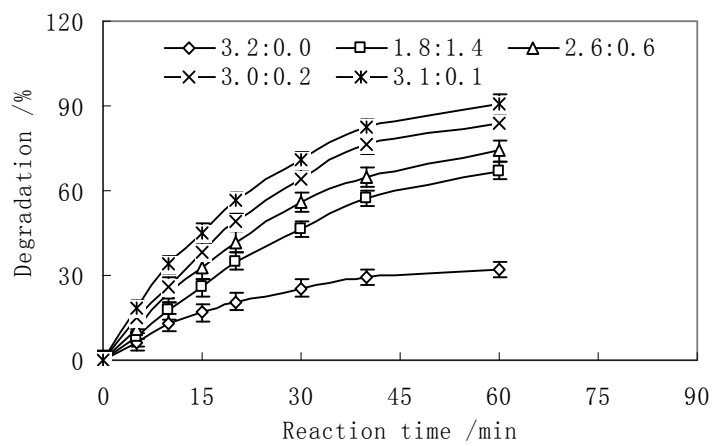
486

487

488

489 Fig. 2.

490



491

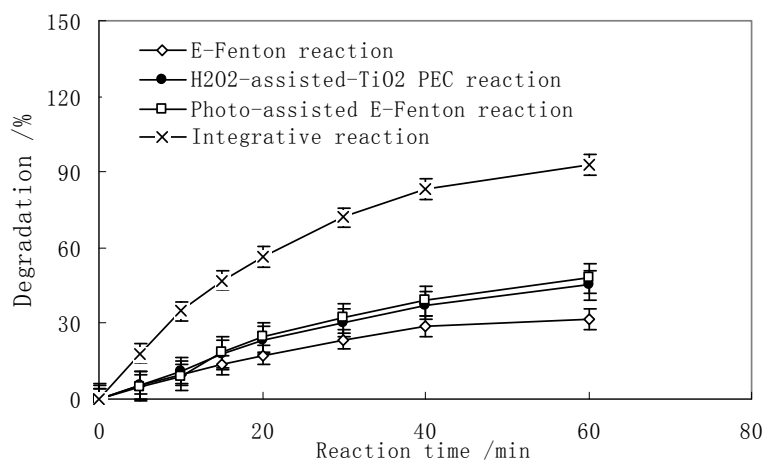
492

493

494

495 Fig. 3.

496



497

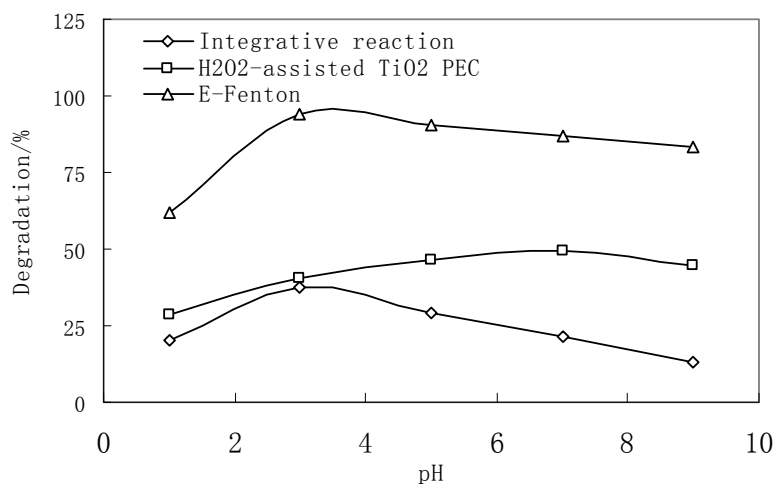
498

499

500 Fig. 4.

501

502



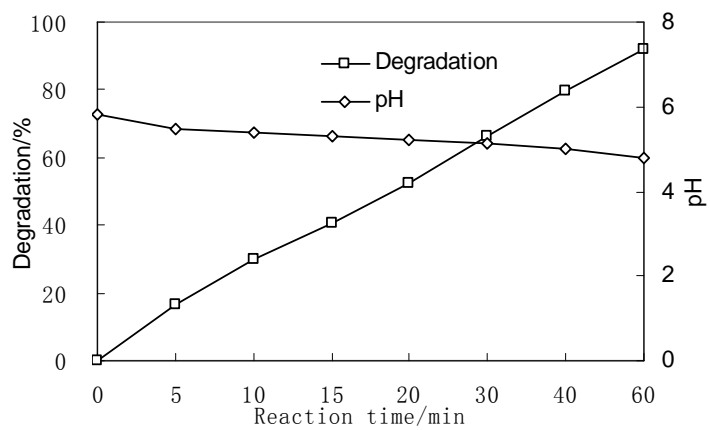
503

504

505

506 Fig. 5.

507



508

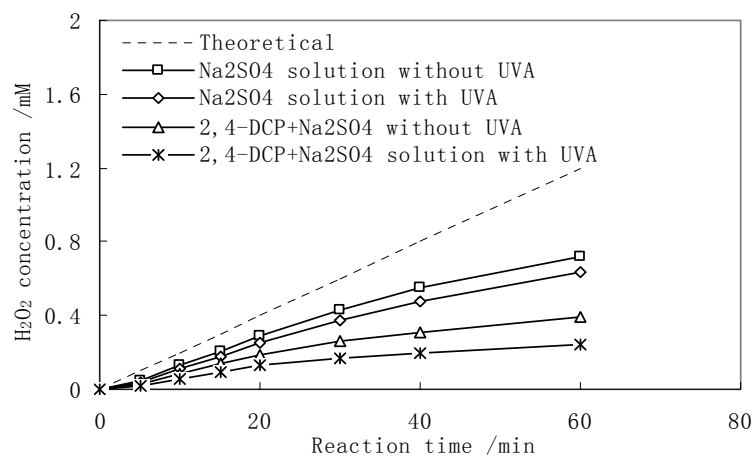
509

510

511

512 Fig. 6.

513



514

515

516

517 Fig. 7.

518

519

520

521

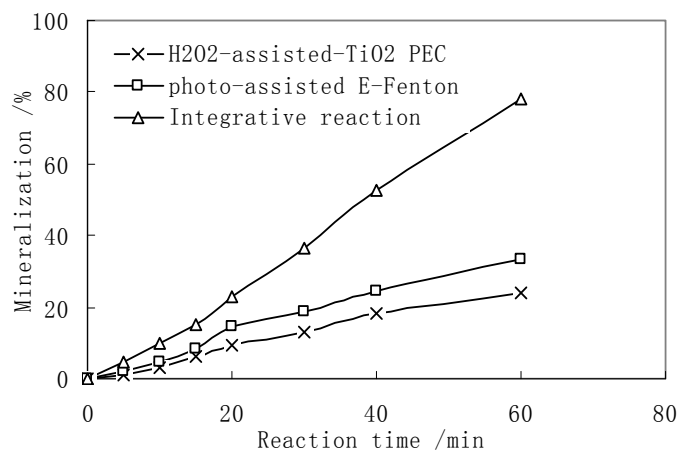
522

523

524

525





526

527

528

529 Fig. 8.

530